UCLA
UCLA Previously Published Works

Title

Dissecting the Mechanism of Histone Deacetylase Inhibitors to Enhance the Activity of Zinc Finger Nucleases Delivered by Integrase-Defective Lentiviral Vectors

Permalink

https://escholarship.org/uc/item/7g26q1fg

Journal

Human Gene Therapy, 25(7)

ISSN

2324-8637

Authors

Joglekar, Alok V
Stein, Libby
Ho, Michelle
et al.

Publication Date

2014-07-01

DOI

10.1089/hum.2013.211

Peer reviewed

Research Articles

Dissecting the Mechanism of Histone Deacetylase Inhibitors to Enhance the Activity of Zinc Finger Nucleases Delivered by Integrase-Defective Lentiviral Vectors

Alok V. Joglekar, Libby Stein, Michelle Ho, Megan D. Hoban,
Roger P. Hollis, and Donald B. Kohn

Abstract

Integrase-defective lentiviral vectors (IDLVs) have been of limited success in the delivery of zinc finger nucleases (ZFNs) to human cells, due to low expression. A reason for reduced gene expression has been proposed to involve the epigenetic silencing of vector genomes, carried out primarily by histone deacetylases (HDACs). In this study, we tested valproic acid (VPA), a known HDAC inhibitor (HDACi), for its ability to increase transgene expression from IDLVs, especially in the context of ZFN delivery. Using ZFNs targeting the human adenosine deaminase (ADA) gene in K562 cells, we demonstrated that treatment with VPA enhanced ZFN expression by up to 3-fold, resulting in improved allelic disruption at the ADA locus. Furthermore, three other U.S. Food and Drug Administration-approved HDACis (vorinostat, givinostat, and trichostatin-A) exhibited a similar effect on the activity of ZFN-IDLVs in K562 cells. In primary human CD34$^+$ cells, VPA- and vorinostat-treated cells showed higher levels of expression of both green fluorescent protein (GFP) as well as ZFNs from IDLVs. A major mechanism for the effects of HDAC inhibitors on improving expression was from their modulation of the cell cycle, and the influence of heterochromatinization was determined to be a lesser contributing factor.

Introduction

INTEGRASE-DEFECTIVE LENTIVIRAL VECTORS (IDLVs) are HIV-1-based vectors packaged with a catalytically inactive integrase (Naldini *et al.*, 1996). When pseudotyped with the vesicular stomatitis virus envelope protein G (VSV-G), IDLVs can transduce a wide variety of human cells efficiently (Vargas *et al.*, 2004). On transduction, IDLV genomic RNA is reverse transcribed to form double-stranded DNA (dsDNA), which is then imported into the nucleus of the host cell as a part of the preintegration complex. The viral genomes exist episomally as 1- or 2-LTR (long terminal repeat) circles or as linear forms, but do not integrate into the chromosome (except at a low level, presumably mediated by nonhomologous end joining). IDLV episomes can act as templates for transcription, supporting the use of IDLVs as expression vectors. Often packaged as self-inactivating (SIN) vectors, IDLV genomic episomes cannot replicate in the host cell. Because the episomes are diluted with each division undergone by the host cell, IDLVs are ideal for transient gene expression. In proliferating cells, IDLV episomes are reduced to background levels within 2–3 weeks post-transduction, allowing gene expression from them to fade away.

The ability to transduce cells efficiently and transiently makes IDLVs ideal gene delivery vectors for the expression of site-specific genome modification reagents (Nightingale *et al.*, 2006). These reagents include nucleases such as zinc finger nucleases (ZFNs) (Urnov *et al.*, 2005), homing endonucleases (Cornu and Cathomen, 2007) TALENs (Christian *et al.*, 2010), and Cas9 nucleases (Cong *et al.*, 2013), which are used to make targeted double-strand breaks (DSBs) in the genome. Once a DSB is made, it is possible to introduce desired genetic modifications near it by manipulating the repair of that break. Nuclease expression, therefore, is required only transiently for this manipulation. Indeed, IDLVs have been investigated for the delivery of homing endonucleases (Cornu and Cathomen, 2007) and ZFNs (Lombardo *et al.*, 2007; Joglekar *et al.*, 2013). Previous reports on the use of IDLVs for ZFN delivery have shown limited success, however, with low levels of gene editing. The efficacy of IDLVs was shown to be severely limited in primary hematopoietic cells. Our previous findings indicate that IDLVs, although efficient at transducing primary hematopoietic cells,

Department of Microbiology, Immunology, and Molecular Genetics; and Eli & Edythe Broad Center of Regenerative Medicine & Stem Cell Research; University of California, Los Angeles, Los Angeles, CA 90095.

do not express sufficient levels of ZFNs for detectable allelic disruption (Joglekar *et al.*, 2013).

One reason proposed for causing low gene expression from IDLVs is their tendency to undergo epigenetic silencing (Pelascini *et al.*, 2013a). Genomes of viruses such as adenoviruses, herpes simplex viruses (HSVs), and retroviruses are known to undergo chromatinization in the nucleus, with histones and other DNA-binding proteins (Lieberman, 2008; Takacs *et al.*, 2010; Knipe *et al.*, 2013). Chromatinization is a mechanism by which a host cell defends against viruses and is accomplished by applying heterochromatin marks on the viral genomes. These heterochromatin marks such as H3K9me3 cause the genomes to be transcriptionally repressed (Lieberman, 2008). This mechanism is responsible for establishing latency of HIV-1 infection, whereby the proviral chromatin is silenced by methylation and deacetylation. The silencing of HIV-1 provirus is mediated by histone deacetylases (HDACs) and histone methyltransferases (HMTs) (Bisgrove *et al.*, 2005; Margolis, 2011). This phenomenon can be reversed by using drugs that act as HDAC inhibitors (HDACis). The use of HDACis results in reactivation of latent HIV-1 infection in T cells (Van Lint *et al.*, 1996), by derepressing the proviral genome. The derepressive effect of HDACis on HIV-1 genomes can be exploited to increase the transgene expression of IDLVs. A study by Pelascini and colleagues showed that IDLV genomes undergo heterochromatinization that can be reversed or prevented by using the HDACi sodium butyrate (NaBu) (Pelascini *et al.*, 2013a). That study reported that NaBu treatment could enhance green fluorescent protein (GFP) reporter gene expression from IDLVs in both dividing and nondividing cells. Another report by the same researchers showed that HDAC inhibitors could be used to increase ZFN expression from IDLVs in cell lines and primary myoblasts (Pelascini *et al.*, 2013b).

In the current study, we used valproic acid (VPA), a U.S. Food and Drug Administration (FDA)-approved HDACi for enhancing ZFN expression from IDLVs. We tested the use of VPA in K562 cells as well as primary human CD34$^+$ hematopoietic stem/progenitor cells (HSPCs) in the context of GFP delivery as well as ZFN delivery from IDLVs. We investigated the effect of three FDA-approved HDACis— vorinostat (VST), givinostat (GST), and trichostatin-A (TSA)—on ZFN expression in IDLV-transduced cells. These studies demonstrate for the first time the use of these HDACis for IDLVs in HSPCs. We also investigated the effects of HDACis on the cell cycle in K562 cells as well as in HSPCs, indicating a stall in the G_1 phase of the cell cycle. These studies identified the cell cycle as another mechanism involved in increasing the efficacy of IDLVs for delivery and expression of ZFNs and other transgenes to HSPCs.

Materials and Methods

HDAC inhibitors

Valproic acid (Sigma-Aldrich, St. Louis, MO) was dissolved in ethanol at a final concentration of 100 mM. Vorinostat, givinostat, and trichostatin-A (Selleckchem, Houston, TX) were dissolved in ethanol at a final concentration of 100 μM. Solutions of the HDAC inhibitors were stored at 4°C.

Cell lines and culture

K562 cells (CCL-243; American Type Culture Collection [ATCC], Manassas, VA) were cultured in RPMI 1640 (Cellgro; Mediatech/Corning, Manassas, VA) supplemented with 10% fetal bovine serum (Gemini Bio-Products, West Sacramento, CA) and penicillin/streptomycin/L-glutamine (Gemini Bio-Products). Human umbilical cord blood samples were collected at the Ronald Reagan UCLA Medical Center (Los Angeles, CA) and as anonymous medical waste have been deemed exempt from institutional review board oversight. Mononuclear cells (MNCs) were isolated from cord blood by Ficoll-Paque (GE Healthcare Biosciences, Piscataway, NJ)-based separation. CD34$^+$ cells were isolated from the MNCs, using a MACS CD34$^+$ enrichment kit (Miltenyi Biotec, Auburn, CA). Genomic DNA from cells was extracted with a PureLink genomic DNA mini kit (Life Technologies/Thermo Fisher Scientific, Waltham, MA) and quantified with NanoVue (GE Healthcare Biosciences). Cells were monitored for mCherry expression with a BD LSRFortessa or BD LSRII flow cytometer (BD Biosciences, San Jose, CA) and analyzed with FlowJo (Tree Star, Ashland, OR). Cell counts were measured with a Vi-CELL XR automated cell counter (Beckman Coulter, Indianapolis, IN).

Transduction of cell lines and primary cells with IDLVs

K562 cells, 1×10^5 per sample, were centrifuged at $90 \times g$ for 10 min and resuspended in 50 μl of culture medium, with or without HDACi, per sample. Appropriate dilutions of viruses were made in culture medium in 50 μl. The diluted virus was added to cells in 48-well tissue culture-treated plates (Corning, Corning, NY). At 2 days post-transduction the cells were transferred to 6-well tissue culture-treated plates (Corning) with 2 ml of culture medium with or without HDACi. CB-CD34$^+$ cells were prestimulated on RetroNectin (Clontech Laboratories, Mountain View, CA)-coated 48-well non-tissue culture-treated plates (Corning) with X-VIVO 15 (Lonza, Walkersville, MD) supplemented with stem cell factor (SCF, 50 ng/ml; Amgen, Thousand Oaks, CA), Flt3 ligand (Flt3L, 50 ng/ml; R&D Systems, Minneapolis, MN), and thrombopoietin (TPO, 50 ng/ml; R&D Systems) for 18 hr at 1×10^5 cells/ml. CB-CD34$^+$ cells were transduced with appropriate dilutions of the virus in X-VIVO 15 with or without the HDACis. At 24 hr post-transduction, cells were transferred to 24-well tissue culture-treated plates (Corning) and maintained in Iscove's modification of Dulbecco's medium (Cellgro IMDM; Mediatech/Corning) with or without HDACis supplemented with 20% fetal bovine serum (Gemini Bio-Products) and stem cell factor (25 ng/ml; Amgen), interleukin (IL)-6 (10 ng/ml; R&D Systems), and IL-3 (5 ng/ml; R&D Systems).

Cell cycle analysis with propidium iodide

K562 cells were transduced with MND-GFP-IDLV as described previously. At 3 days post-transduction, cells were harvested by centrifugation at $300 \times g$ for 5 min. The cells were resuspended in 100 μl of Dulbecco's phosphate-buffered saline (DPBs) with 1% fetal bovine serum, followed by addition of 700 μl of ice-cold ethanol with gentle vortexing. The cells were kept at -20°C overnight and then washed twice with DPBS. Cells were then incubated with

FxCycle PI/RNase staining solution (Life Technologies/ Thermo Fisher Scientific) for 30 min at room temperature in the dark and analyzed by flow cytometry.

Western blotting for analysis of ZFN expression

ZFN expression was monitored by Western blotting for FLAG-tag, which is present at the amino terminus of both ZFN proteins. Lysates from cells transduced with the ZFN vectors were produced with denaturing cell extraction buffer (Life Technologies/Thermo Fisher Scientific) supplemented with complete mini protease inhibitor tablets (Roche Applied Science, Indianapolis, IN). Cells were centrifuged at $500 \times g$ for 10 min at 4°C and the supernatant was aspirated. The cell pellets were resuspended in 50 μl of lysis buffer per 1×10^6 cells and incubated on ice for 45 min with frequent vortexing. The lysate was centrifuged at $16,000 \times g$ for 20 min at 4°C. The supernatant was transferred to fresh tubes and stored at -20°C until further use. The protein quantities were estimated by bicinchoninic acid (BCA) assay (Pierce Biotechnology/Thermo Fisher Scientific, Rockford, IL) and read on an Infinite M1000 microplate reader (Tecan, Morrisville, NC). Equal amounts of protein lysate (40 μg/lane) combined with Laemmli sample buffer (Bio-Rad, Hercules, CA) were loaded on 4–12% Bis-Tris sodium dodecyl sulfate (SDS)–polyacrylamide gels (Life Technologies/Thermo Fisher Scientific). Each gel was run at 150 V for 1 hr in 1× 3-(N-morpholino)propanesulfonic acid (MOPS)–SDS running buffer (Life Technologies/Thermo Fisher Scientific) in a Novex gel electrophoresis unit (Life Technologies/Thermo Fisher Scientific). Prism Ultra (Abcam, Cambridge, MA) protein standards were loaded for size determination. The proteins were transferred from the gel to a polyvinylidene difluoride (PVDF) membrane (Life Technologies/Thermo Fisher Scientific) in 1× Novex transfer buffer with 10% methanol (Life Technologies/Thermo Fisher Scientific). The transfer was carried out at 30 V for 1 hr at room temperature. After the transfer, the membrane was blocked with 5% nonfat milk in PBS–Tween 20 for 30 min at room temperature. After blocking, the membrane was incubated with 1:1000 diluted mouse anti-FLAG primary antibody (Sigma-Aldrich) overnight at 4°C. The membrane was then washed three times with PBS–Tween 20 and incubated with a 1:5000 dilution of goat anti-mouse IgG–horseradish peroxidase (HRP) secondary antibody (Sigma-Aldrich) for 3 hr at room temperature. The membrane was washed again three times with PBS–Tween 20. The membrane was incubated at room temperature with ECL2 reagent (Pierce Biotechnology/Thermo Fisher Scientific) for 5 min and imaged with a Typhoon FLA 9500 phosphorimager (GE Healthcare Biosciences).

Chromatin immunoprecipitation

Cross-linked chromatin from 3×10^6 cells per sample was prepared with a truChIP low cell chromatin shearing kit with SDS shearing buffer according to the manufacturer's instructions (Covaris, Woburn, MA). Chromatin was sheared with a Covaris sonicator for 4 min according to the manufacturer's instructions. Sheared chromatin was immunoprecipitated with the MAGnify chromatin immunoprecipitation system according to the manufacturer's instructions (Life Technologies/ Thermo Fisher Scientific). ChIP-grade antibodies anti-histone

H3 (tri methyl K4) and anti-histone H3 (tri methyl K9) (Abcam) were used for immunoprecipitation. The concentration of the pulled-down chromatin was quantified with Pico-Green (Life Technologies/Thermo Fisher Scientific). Equal amounts of chromatin, 3 μl, were added to 100 μl of 1× PicoGreen and quantified on an Infinite M1000 plate reader (Tecan). The immunoprecipitated chromatin was then analyzed via quantitative PCR (qPCR), using SYBR green PCR master mix (Applied Biosystems, Warrington, UK) and MND-forward (5′-CCTGAAATGACCCTGTGCCTT-3′) and MND-reverse primers (5′-AGGGGTTGTGGGCTCTTTTAT-3′). The qPCR was run at the default settings on the ViiA 7 thermal cycler (Applied Biosystems).

Surveyor nuclease assay

The Surveyor nuclease assay was used to determine ZFN-induced site-specific allelic disruption. A 332-bp region surrounding the ZFN-binding site was amplified from 200 ng of genomic DNA, using 474F (5′-CTACCTGACACATGGTAA CTGGCTAATGAG-3′) and 474R (5′-AATAGAGCCAAGT ATGGGAGGAGGCAGTGAGGAGGG-3′) and AccuPrime *Taq* DNA Polymerase High Fidelity (Life Technologies/ Thermo Fisher Scientific) under the following conditions: 94°C for 2 min followed by 30 cycles of 94°C for 30 sec, 62°C for 30°C sec, and 68°C for 1 min, followed by a final extension of 68°C for 5 min. The PCR product was diluted 1:2 in 6 μl of 1× AccuPrime buffer and subjected to denaturation and reannealing under the following conditions: 94°C for 10 min, followed by cooling to 85°C at -2°C/sec and cooling to 25°C at -0.1°C/sec. The reaction mixture was then digested with 1 μl of Surveyor nuclease (Transgenomic, Omaha, NE) at 42°C for 15 min. The reactions were resolved on 8% Tris–borate–EDTA (TBE)–polyacrylamide gels (Life Technologies/Thermo Fisher Scientific) at 120 V for 45 min. The gels were removed from the cassettes and stained with 5 μl of GelGreen (Phenix Research Products, Candler, NC) in 50 ml of 1× TBE for 15 min and imaged on a Kodak Gel Logic 212 Imaging System (Brucker Corp., Billerica, MA). The gel images were analyzed by densitometry and allelic disruption was determined according to the following formula:

$$\%\text{Allelic disruption} = 100 \times (1 - [\text{intensity of uncut band} / \text{total intensity of cut and uncut bands}]^{1/2})$$

Colony formation assay

Human primary $CD34^+$ HSPCs were transduced with either MND-GFP-IDLV or MND-ZFN-IDLV and treated with HDAC inhibitors. At 4 days post-transduction, 100 or 300 cells were plated on gridded plates (Thermo Scientific, Roskilde, Denmark) in 1 ml of MethoCult-enriched methylcellulose medium with recombinant cytokines for human cells (StemCell Technologies, Vancouver, BC, Canada). The plates were incubated at 37°C for 2 weeks. Colonies were counted manually and classified according to their phenotype.

Statistical analysis

An unpaired Student's *t* test was performed to compare individual drug treatments. Linear regression on log–log

transformations was performed on relative fold expansion and relative transgene expression to calculate the R^2 values. All statistical analyses were done with GraphPad Prism (GraphPad Software, La Jolla, CA).

Results

Valproic acid enhances gene expression from IDLVs in K562 cells

To investigate the use of VPA to increase gene expression from IDLVs, K562 cells were transduced with an IDLV expressing GFP under the control of a modified myeloproliferative sarcoma virus LTR (MND-GFP-IDLV). The cells were treated with 1 mM VPA, and GFP expression and cell viability were measured every day for 4 days. Enhancement of GFP expression in VPA-treated cells was evident from day 2 post-transduction, reaching its peak on day 3 post-transduction, when VPA-treated cells showed 2.5-fold higher mean fluorescence intensity (MFI) of GFP expression compared with the control cells. Overall cell viability

was not affected significantly ($p > 0.01$) at any time point, suggesting that VPA treatment does not exhibit acute cytotoxicity (Fig. 1a).

We hypothesized that the effect of VPA on gene expression can be exploited to enhance the efficacy of ZFNs delivered by IDLVs. To test this, we used a previously published set of ZFNs targeting intron 6 of the human adenosine deaminase (ADA) gene (Joglekar *et al.*, 2013). We used IDLVs coexpressing two ZFNs under the control of either the intron-deleted human elongation factor-1a promoter (EFS) or the MND promoter with a downstream mCherry reporter gene linked by a 2A sequence. The ZFN target sites and the vector constructs are shown in Supplementary Fig. S1 (Supplementary Data are available online at www.liebertpub.com/hum). We transduced K562 cells with EFS-ZFN-IDLV or MND-ZFN-IDLV, treated them with 1 mM VPA or vehicle, and analyzed them 4 days later. Flow cytometry showed that mCherry expression significantly increased ($p < 0.01$) with VPA treatment (Fig. 1b). The increase was more with MND-ZFN-IDLV (2.7-fold) than with
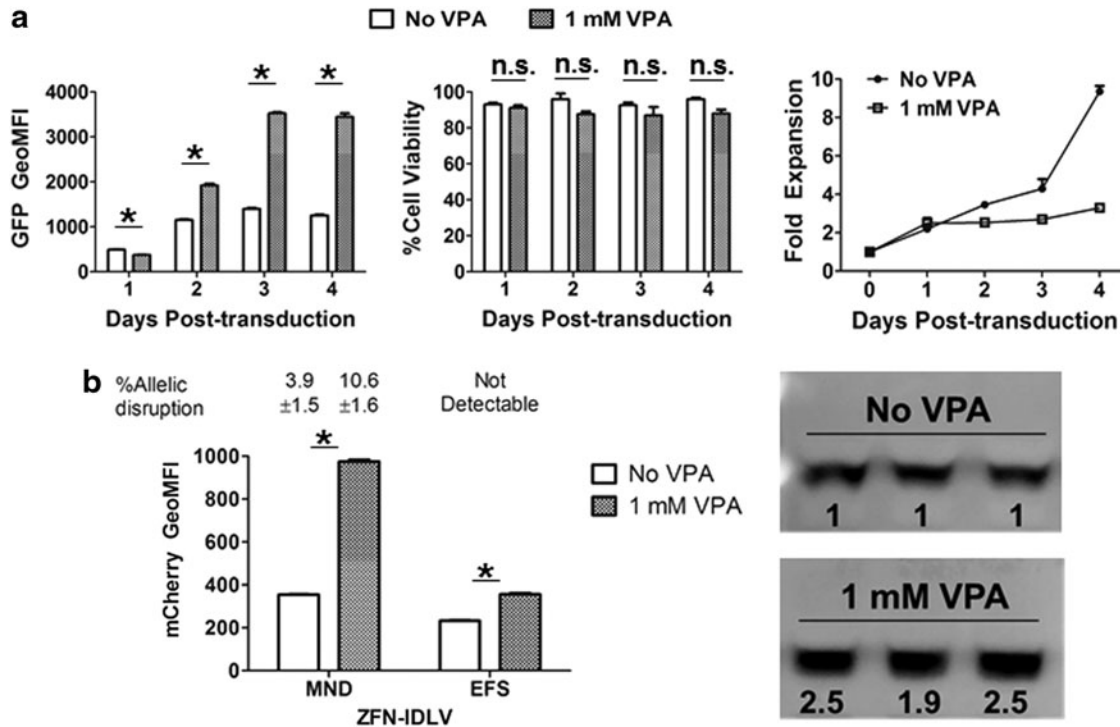

FIG. 1. Valproic acid (VPA) enhances gene expression from integrase-defective lentiviral vectors (IDLVs) in K562 cells. **(a)** *Left:* Effect of VPA on green fluorescent protein (GFP) expression from IDLVs. Geometric mean fluorescence intensity (GeoMFI) at various time points post-transduction is plotted on the *y* axis. *Middle:* Effect of VPA on cell viability. Percentage of viable cells at each time point post-transduction is plotted on the *y* axis. Open columns indicate untreated cells, whereas shaded columns indicate cells treated with 1 mM VPA. *Right:* Effect of VPA on cell expansion. Fold cell expansion at each time point post-transduction is plotted on the *y* axis. Circles indicate untreated cells; squares indicate cells treated with 1 mM VPA. All values are represented as means ± SD ($n = 3$). Significance of results is indicated by asterisk (*$p < 0.01$); n.s., not significant. **(b)** *Left:* Effect of VPA on zinc finger nuclease (ZFN)-IDLVs. Shown is the expression of mCherry reporter from ZFN-IDLVs in K562 cells 4 days post-transduction. The *y* axis represents the geometric MFI of mCherry. The numbers above the columns indicate percent allelic disruption from these samples. Open columns indicate untreated cells, whereas shaded columns indicate cells treated with 1 mM VPA. Columns and numbers represent means ± SD ($n = 3$). Statistical significance is indicated by asterisks (*$p < 0.01$). *Right:* Western blot to show the effect of VPA treatment on ZFN expression. Cells were transduced with MND-ZFN-IDLV and collected 4 days post-transduction. Cell lysates were blotted with an antibody against FLAG-tag, which is present at the amino terminus of both ZFN proteins. *Top:* Untreated samples. *Bottom:* Samples treated with 1 mM VPA. The numbers under the bands indicate ZFN expression per cell, normalized to matched, untreated samples.

EFS-ZFN-IDLV (1.5-fold). The increase in mCherry reporter gene expression was also associated with a 2.7-fold increase in allelic disruption at the ZFN cleavage site in the ADA gene with MND-ZFN-IDLV. EFS-ZFN-IDLV did not induce detectable allelic disruption even after treatment with VPA. Western blotting for the FLAG-tag present in the ZFN-encoding genes confirmed up to a 2.5-fold increase in ZFN protein expression on VPA treatment (Fig. 1b). These results demonstrate that VPA treatment can be used to enhance ZFN expression from IDLV in K562 cells.

Valproic acid enhances gene expression from IDLVs in human HSPCs

We investigated whether VPA treatment could provide a viable way to increase gene expression from IDLVs in primary human HSPCs, as we had previously observed that expression of ZFN from IDLV in these cells was too low to exhibit detectable allelic disruption (Joglekar *et al.*, 2013). We isolated CD34$^+$ HSPCs from umbilical cord blood, prestimulated them with cytokines for 24 hr, and transduced them with MND-GFP-IDLV in the presence or absence of VPA. Flow cytometry 4 days post-transduction showed in-

creased intensity of GFP expression and a concordant elevation in the percentage of GFP$^+$ cells in a dose-dependent response with increasing VPA concentrations. At its maximum (at 1.5 mM VPA), the GFP expression per cell increased by 1.9-fold and the percentage of GFP$^+$ cells increased by 1.4-fold (Fig. 2a).

On the basis of previous results in K562 cells, we analyzed the cell proliferation of HSPCs on VPA treatment. We found that 4 days post-transduction, there was no obvious reduction in percent viability, but there was up to 2-fold reduction in cell expansion. The reduction in cell expansion also showed a correlation with VPA concentration (Fig. 2b). To assess whether treatment with VPA affected the differentiation potential of the HSPCs, we performed a methylcellulose-based colony-forming unit (CFU) assay with the cells 4 days post-transduction. Analysis of colonies formed after 2 weeks of culture in methylcellulose revealed that VPA treatment reduced the number of colonies arising from these cells, by up to 3-fold (Fig. 2b). The relative proportion of colonies of various lineages did not show a significant difference (Supplementary Fig. S2). These findings indicate that although VPA treatment did not affect the differentiation capacity of the HSPCs, it decreased the percentage that could
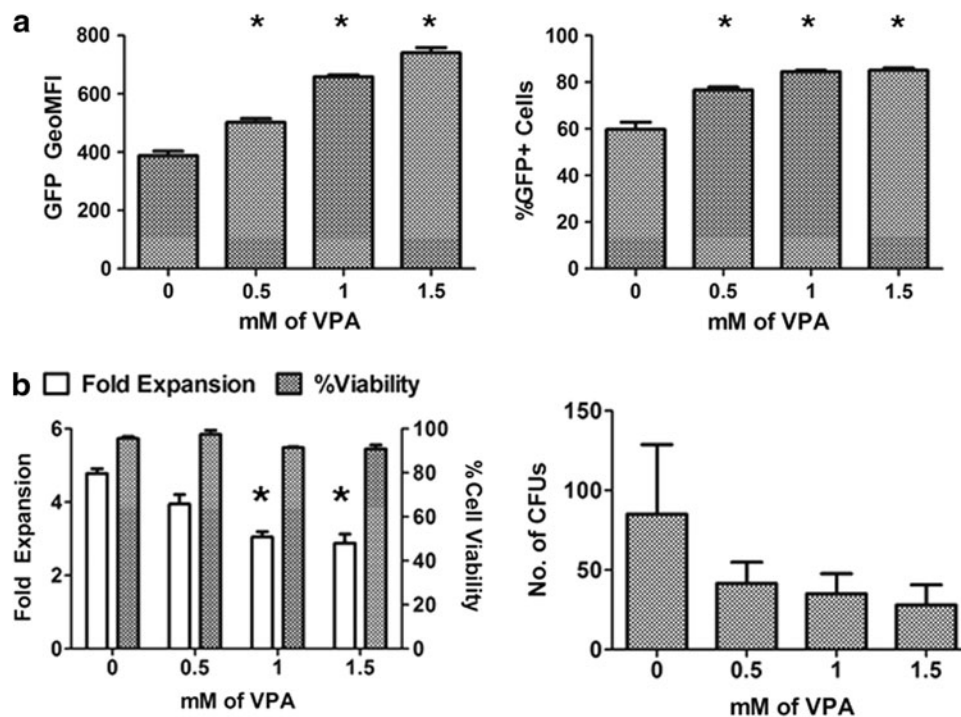

FIG. 2. Valproic acid enhances gene expression from IDLVs in human hematopoietic stem/progenitor cells (HSPCs). **(a)** *Left:* Effect of VPA treatment on GFP expression from IDLVs in human HSPCs. Shown is the effect of VPA treatment on the geometric MFI of GFP in human HSPCs 4 days post-transduction. The *y* axis indicates GFP geometric MFI, and the *x* axis indicates concentration of VPA (mM). *Right:* Effect of VPA treatment on the percentage of GFP$^+$ human HSPCs 4 days post-transduction. The *y* axis indicates percent GFP$^+$ cells, and the *x* axis indicates the concentration of VPA used (mM). Numbers represent means $\pm$ SD ($n = 3$). Statistical significance is indicated by asterisks (*$p < 0.01$). **(b)** Effect of VPA treatment on survival of HSPCs. *Left:* Effect of VPA treatment on cell viability and expansion 4 days post-transduction. Open columns indicate fold expansion relative to cell number at the time of transduction, plotted on the left *y* axis. Shaded columns indicate the percentage of viable cells, plotted on the right *y* axis. The *x* axis indicates concentrations of VPA (mM). *Right:* Effect of VPA on the differentiation potential of HSPCs. The *y* axis indicates the number of colony-forming units (CFUs) seen after 14 days of culture in methylcellulose, starting with equal numbers of cells 4 days post-transduction. The *x* axis indicates concentrations of VPA (mM). Columns indicate means $\pm$ SD ($n = 3$). Statistical significance is indicated by asterisks (*$p < 0.01$).

form colonies. This may indicate a potential delayed toxicity on the cells that is not apparent at 4 days post-transduction.

FDA-approved HDAC inhibitors enhance gene expression from IDLVs

We sought to determine whether HDACis other than VPA would be able to enhance gene expression from IDLVs, while reducing the cytostatic effect. Therefore, we investigated the FDA-approved HDACis vorinostat (VST), givinostat (GST), and trichostatin-A (TSA) for their effect on MND-ZFN-IDLV in K562 cells. Flow cytometry revealed that VST, GST, and TSA enhanced mCherry signal from the IDLV. The fold increase in mCherry expression was most dramatic in GST-treated cells (20-fold). ZFN activity as measured by Surveyor nuclease assay did not correlate with such high levels of mCherry expression. HDACi-treated cells showed a 2- to 4-fold increase in percent allelic disruption, with VPA showing the highest effect (Fig. 3a). Similar to VPA treatment, VST, GST, and TSA reduced cell

expansion dramatically: whereas VST did not affect cell viability as dramatically, GST and TSA reduced it by 30% (Fig. 3a).

We also tested the FDA-approved HDACis for their effect on ZFN-IDLV in primary human CD34^{+} HSPCs. We found that TSA and GST were highly cytotoxic (viable cell counts under the detection limit), but VST did not show acute cytotoxicity. Flow cytometry of VPA- and VST-treated cells revealed a moderate increase in mCherry signal and in percent mCherry^{+} cells (Fig. 3b). Surveyor nuclease assays did not reveal detectable allelic disruption in these cells, suggesting that the ZFN expression levels were still insufficient. This increase in mCherry signal was also associated with reduced cell proliferation. To assess whether the cytostatic effect of VPA and VST could result in delayed toxicity, we performed colony formation assays on HDACi-treated HSPCs and found that both VPA and VST reduced the total number of CFUs (Fig. 3b). These data could be attributed to the possible delayed toxicity of these HDACis, which is not seen at the time of viability assessment.
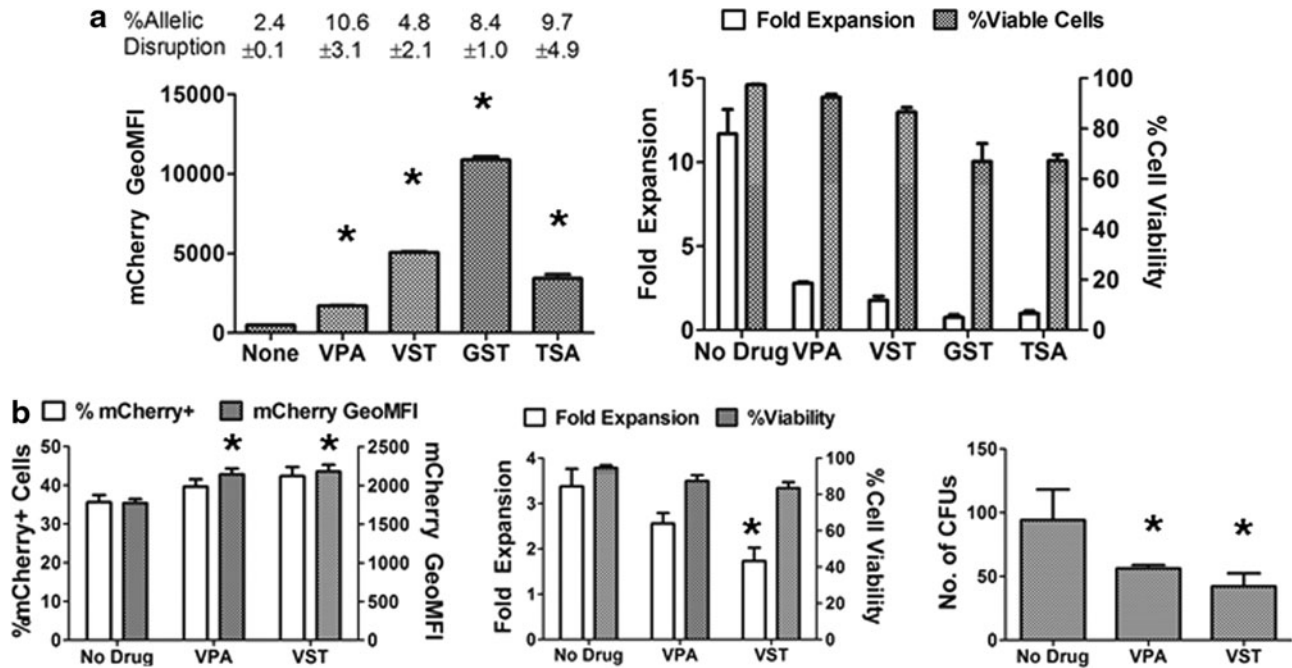

FIG. 3. FDA-approved HDAC inhibitors (HDACis) enhance gene expression from IDLVs. **(a)** Effect of FDA-approved HDACi on gene expression from ZFN-IDLVs in K562 cells. *Left:* Expression of mCherry reporter from ZFN-IDLVs in K562 cells 4 days post-transduction. The y axis represents the geometric MFI of mCherry. Numbers above the columns indicate percent allelic disruption from these samples. The x axis represents the HDACi used. *Right:* Effect of HDAC inhibitors on survival of K562 cells 4 days post-transduction. Open columns indicate fold expansion relative to cell number at the time of transduction, plotted on the left y axis. Shaded columns indicate percentage of viable cells, plotted on the right y axis. Columns and numbers represent means ± SD ($n = 3$). Statistical significance is indicated by asterisks (*$p < 0.01$). **(b)** Effect of VPA and vorinostat (VST) on ZFN-IDLVs in human HSPCs. *Left:* Effect of VPA and VST on gene expression from MND-ZFN-IDLV in human HSPCs 4 days post-transduction. Open columns indicate the percentage of mCherry-expressing cells, plotted on the left y axis; shaded columns indicate the geometric MFI of mCherry, plotted on the right y axis. *Middle:* Effect of HDAC inhibitors on survival of human HSPCs 4 days post-transduction. Open columns indicate fold expansion relative to cell number at the time of transduction, plotted on the left y axis. Shaded columns indicate the percentage of viable cells, plotted on the right y axis. *Right:* Effect of VPA on the differentiation potential of HSPCs. The y axis indicates number of colony-forming units (CFUs) seen after 14 days of culture in methylcellulose, starting with equal numbers of cells 4 days post-transduction. The x axis indicates the HDAC inhibitor used (VPA corresponds to 1 m*M* VPA, VST corresponds to 1 μ*M* VST). Columns indicate means ± SD ($n = 3$). Statistical significance is indicated by asterisks (*$p < 0.01$).

*Mechanism of VPA- and VST-mediated enhancement
of gene expression*

We sought to determine the mechanism by which VPA and VST affect gene expression. Previous studies have suggested that HDAC inhibitors alter the chromatin state of the IDLV genomes, thereby increasing transgene expression (Pelascini *et al.*, 2013a). If VPA and VST were acting in this manner by affecting the net gene expression per vector genome, there should be an increase in reporter gene signal per vector copy in treated cells. On the basis of the vector copy number and the GFP signal, we observed that there was no significant increase in MFI per vector copy for either VPA ($p = 0.46$) or VST ($p = 0.15$). Although not statistically significant, VPA treatment showed a slight increase in MFI per vector copy. These results suggest that there may be an additional mechanism for the effect of VPA and VST (Fig. 4a).

We performed chromatin immunoprecipitation on K562 cells transduced with MND-GFP-IDLV and treated with VPA or VST. We probed for enrichment of the open chromatin marker H3K4me3 and the closed chromatin marker H3K9me3 at the MND promoter in these cells. We found

that VPA caused a reduction of enrichment of both these marks as compared with vehicle. The dramatic decrease in enrichment of H3K9me3 in VPA-treated cells suggests reduction of heterochromatinization at the MND promoter. In contrast to VPA, VST showed only slight changes at both marks, with a slight increase in the enrichment at H3K4me3 and a slight decrease in enrichment at H3K9me3 (Fig. 4b). These results support a previous observation (Pelascini *et al.*, 2013a,b) that one of the ways by which VPA enhances gene expression is due to its effects on the chromatin state.

We investigated whether the previously observed cytostatic effect of VPA or VST contributed to the enhancement of gene expression from IDLVs in K562 cells. We analyzed the cell cycle stage of transduced and HDACi-treated cells by staining them with propidium iodide. At 3 days post-transduction, the majority of cells treated with VPA were in the G_1 phase (73%), compared with untreated cells (47%). This observed cell cycle arrest would explain the cytostatic effect on the cells. On the other hand, VST-treated cells showed no difference in the fraction of cells in G_1 phase (51%) compared with untreated cells. These results would suggest that VPA exerts a greater cytostatic effect on
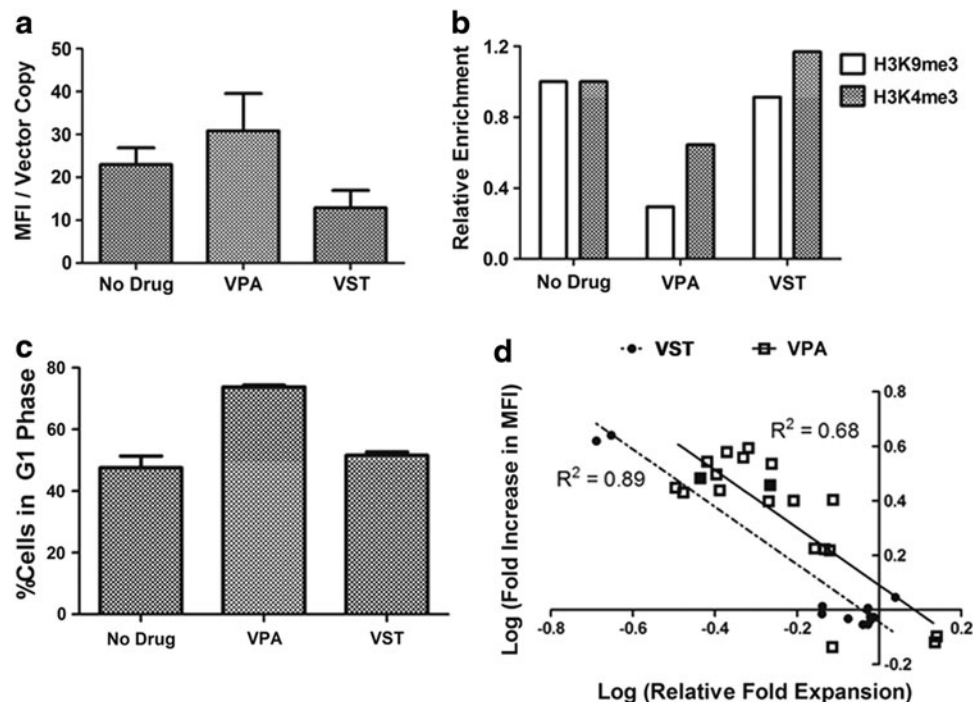

FIG. 4. Mechanism of action of HDAC inhibitors. **(a)** Effect of HDAC inhibitors on MND-GFP viral genomes in K562 cells. Shown is the effect of VPA and VST on gene expression per vector copy 4 days post-transduction. The *y* axis represents the GFP geometric MFI per vector copy, and the *x* axis indicates the HDACi used. The columns represent means $\pm$ SD ($n = 3$). **(b)** Effect of VPA and VST on chromatin state of the MND promoter in K562 cells. K562 cells transduced with MND-GFP and treated with HDAC inhibitors were subjected to chromatin immunoprecipitation, using antibodies against closed chromatin marker H3K9me3 (open columns) or open chromatin marker H3K4me3 (shaded columns). The enrichment of these marks at the MND promoter was quantified by qPCR and is presented relative to the untreated control on the *y* axis. **(c)** Effect of HDAC inhibitors on the cell cycle of K562 cells. K562 cells were transduced with MND-GFP-IDLV and treated with HDAC inhibitors. Cells were stained with propidium iodide (PI) 3 days post-transduction. The *y* axis represents the percentage of cells in the G_1 phase according to PI staining. The *x* axis represents the HDAC inhibitor used. **(d)** Relationship between gene expression and cell expansion in K562 cells. Log-transformed values for the increase in MFI and cell expansion relative to matched, untreated samples are plotted for various samples from either VPA-treated cells (squares) or VST-treated cells (circles). Linear regression analysis was performed and the trend lines are represented for VPA treatment (solid line) and VST treatment (dotted line). The R^2 values indicating goodness of fit are shown.

cells than VST, thereby partly explaining our observations of a greater increase in expression from IDLV by VPA than by VST.

Because IDLV genomes are not replication competent and are diluted by cell division, vector copy number per cell will be inversely proportional to cell expansion. If there is no effect on expression per vector copy, the increase in transgene expression per cell will also be inversely proportional to cell expansion. Therefore, the log–log transformed values of gene expression per cell and cell expansion relative to untreated cells would show a linear relationship (a straight line with slope = −1 and passing through the origin). We plotted the log–log transformations of the observed values of increase in gene expression per cell against relative cell expansion in VPA- and VST-treated cells. We found that values from VPA-treated cells moderately fit a straight line ($R^2 = 0.68$, $p < 0.01$) with a slope of −1.054 and y intercept of 0.09. On the other hand, VST-treated cells fit the straight-line model ($R^2 = 0.89$, $p < 0.01$) with a slope of −1.056 and y intercept of −0.04. The observation that these values fit a linear model indicates that the cytostatic effect of the HDAC inhibitors is a major mechanism behind enhancing IDLV expression in K562 cells (Fig. 4d). Taken together, these data suggest that the action of VPA is due to both its effect on viral chromatin as well as its cytostatic effect. However, these data are not able to sufficiently explain the effects of VST on cells.

Discussion

The use of IDLVs for delivery of ZFNs and other transgenes has been reported previously (Lombardo *et al.*, 2007; Staunstrup and Mikkelsen, 2011). Although IDLVs permit efficient and nontoxic transient transduction of human cells, they do not express transgenes at high levels (Joglekar *et al.*, 2013), which is especially critical for delivery of genome-editing reagents such as ZFNs, where the genome-editing event may be achieved by a short burst of expression of the genome-modifying nuclease. We previously showed that IDLVs could be used to deliver ZFNs to K562 cells as well as to primary human HSPCs. However, low ZFN expression levels severely limited their use as a delivery method. In that study, we showed that there was no detectable gene disruption in HSPCs transduced with ZFN-IDLVs. Therefore, we sought to use this system to assess a potential way to increase ZFN expression from IDLVs. A study showed that low expression levels from IDLVs could be due to epigenetic control of their transcription (Pelascini *et al.*, 2013a,b). IDLV genomes were shown to undergo heterochromatinization, which is mediated mainly by HDACs and may be a cellular defense mechanism against viruses. Heterochromatinization, that is, acquisition of transcriptionally repressive chromatin marks, on IDLVs reduces their transcription, causing low expression. The report by Pelascini and colleagues also showed that this heterochromatin effect suppressing expression by IDLV could be reversed by using sodium butyrate, an HDACi. A report by the same researchers built on this study by using HDACis to enhance ZFN expression in human cell lines as well as myoblasts (Pelascini *et al.*, 2013b).

We investigated whether valproic acid could be used to enhance ZFN expression by IDLVs. To that end, we used a previously published strategy for allelic disruption of the human adenosine deaminase (ADA) gene (Joglekar *et al.*, 2013). We showed that treatment with VPA could enhance gene expression from IDLVs in K562 cells both in the context of GFP and ZFN delivery. The increase in ZFN expression also caused an increase in allelic disruption at the ADA locus. These results demonstrate the usefulness of VPA in improving ZFN expression from IDLVs. We tested this approach in human HSPCs and found that VPA could enhance gene expression from IDLVs in HSPCs as well, although to a lesser extent. In addition to VPA, we tested three other FDA-approved HDACis (VST, GST, and TSA) for their efficacy on IDLVs. We showed that all three performed better than VPA to increase expression levels in K562s when used with either a GFP-IDLV or ZFN-IDLV. Although VPA produced the least dramatic increase in mCherry signal from ZFN-IDLV, it produced the highest degree of allelic disruption in K562 cells.

To determine whether there is any potential benefit of HDACi treatment in a clinically relevant cell type, we tested them in the context of ZFN delivery in primary CD34^{+} HSPCs. VPA and VST were able to enhance mCherry signal from IDLVs, although less dramatically than in K562 cells. Our data support the hypothesis that HDACi treatment increases transgene expression per se from IDLVs in HSPCs; however, there was still insufficient ZFN expression to result in detectable disruption at the ADA locus. This observation was not just limited to the set of ZFNs targeting ADA, which are not efficient (Joglekar *et al.*, 2013); repeating these experiments using highly efficient ZFNs also resulted in no detectable gene disruption in primary cells (data not shown). These data suggest that IDLVs may still be too limited as a delivery method for ZFNs in CD34^{+} cells, despite their enhanced ZFN expression resulting from treatment with VPA and VST.

Although the HSPCs may not be a suitable model for specifically analyzing enhanced ZFN expression from IDLVs after HDACi treatment, reporter gene expression was enhanced and there were other important observations made during these experiments. For example, GST and TSA exhibited significant cytotoxicity, whereas VPA and VST exhibited a cytostatic effect. We showed that treatment with either VPA or VST reduced the overall colony-forming capacity of HSPCs. This could be due either to the effects of VPA on differentiation capacity or to delayed toxicity. In this study, we treated HSPCs with VPA/VST for 4 days and withdrew the treatment before plating them in methylcellulose-containing medium. The cellular changes caused by the HDACis may have a long-term impact on the cells. It has been reported previously that VPA causes selective expansion of CD34^{+} HSPCs, leading to increased CFUs as well as increased engraftment *in vivo* (Burba *et al.*, 2011; Kaur *et al.*, 2013). However, the VPA concentrations used in those studies were four to five times lower than the concentrations used in our study. Although VPA may have positive effects on HSPCs at lower concentrations, at the concentrations that enhance IDLVs VPA decreased the colony-forming potential. Neither VPA nor VST shows significant acute toxicity (4 days post-transduction) as evident from the high cell viability seen at this time point. However, the 4-day-long treatment may impose unwanted effects on HSPCs that cause delayed toxicity. Whether the

delayed effect is caused by chromatin modifications or is due to cytostatic effects is not clear. It may be possible that these two causes are indistinguishable, as they could be linked to each other. These issues regarding adverse effects of VPA/VST need to be addressed if these HDACis are to be used in primary cells. Studies have indicated that *ex vivo* culture of HSPCs using standard cytokines (SCF, Flt3L, TPO, and IL-3) and VPA can increase the reconstitution potential of severe combined immunodeficiency (SCID)-repopulating cells (Bug *et al.*, 2005, De Felice *et al.*, 2005). However, if these inhibitors are to be used during *ex vivo* manipulation of HSPCs, thorough analyses assaying for delayed cytotoxicity need to be performed. At a minimum these analyses should include hematopoietic colony formation assays as well as SCID mouse repopulation assays, ensuring that HDACi treatment does not perturb hematopoiesis compared with untreated controls.

Cytostatic effects of HDACis are a well-known phenomenon, and may be one of the mechanisms contributing to their anticancer activity. The reduction in cell proliferation by HDACis has significant consequences for using IDLVs for transgene delivery. Because IDLV genomes are diluted out with cell division, reduced cell proliferation would cause cells to retain more IDLV genomic copies, leading to more transgene expression per cell. Our data regarding cell proliferation and vector copy number measurements support this contention. We reasoned that if the drug treatment has no effect on gene expression per vector copy, total transgene expression should be inversely proportional to cell proliferation. The log transformations of these parameters form a straight line, intersecting the origin. We plotted the observed values of these two parameters in K562 cells from four different experiments. We found that the observations for both VPA treatment and VST treatment fit a linear model. This correlation would suggest strongly that inhibition of cell proliferation plays a major role in enhancing gene expression in IDLV-transduced cells. One interesting observation from these results is that the *y* intercept of the line representing the observed values for VPA is not zero. This would indicate that even without any change in cell proliferation, there could still be a small increase in gene expression (1.2-fold). This effect may represent the effects of VPA on chromatin. We observed that VPA treatment did indeed reduce the presence of heterochromatin marks (H3K9me3) on the MND promoter. These results are in partial agreement with those observed by Pelascini and colleagues. Their study did not address cell proliferation affecting IDLVs; they attributed the effect of HDACis to chromatin modifications (Pelascini *et al.*, 2013b). On the basis of our results, we propose that both chromatin modifications and decelerated cell proliferation are responsible for enhancing IDLV-mediated gene expression. Although both these effects are seen in K562 cells and HSPCs, there are differences between the efficacies of HDAC inhibitors in these cells. This could be due to differences in HDAC activity present in these cell types. A study by Wada and colleagues showed that HDAC1 and HDAC3 expression differs between K562 cells and bone marrow-derived CD34$^+$ cells. They also showed that HDAC1 expression is important in determining the differentiation program of CD34$^+$ cells (Wada *et al.*, 2011). This could also explain the differences between the efficacies of

VPA and VST. The IC$_{50}$ of VPA and VST vary greatly with different HDACs (Huber *et al.*, 2011). Therefore, for each cell type under consideration, a multitude of HDAC inhibitors should be tested.

In summary, we found that HDAC inhibitors, particularly VPA, could enhance the capacity of IDLVs for expressing transgenes in cell lines or primary hematopoietic cells. We successfully tested the usefulness of this effect for ZFN delivery by IDLVs. Although we found this approach to work reasonably well in K562 cells, it was still insufficient for producing high levels of ZFNs in primary HSPCs. We also determined that HDACis affect cell proliferation and that this phenomenon plays a major role in their effect on the levels of expression from IDLVs. Our data build on previous findings and demonstrate that the mode of action of HDACis is a combination of their cytostatic effect and their effect on viral chromatin. These studies further support the application of HDACis for enhancing IDLV-mediated delivery of ZFNs and other transgenes.

Acknowledgments

Author Disclosure Statement

No competing financial interests exist.

References

Bisgrove, D., Lewinski, M., Bushman, F., and Verdin, E. (2005). Molecular mechanisms of HIV-1 proviral latency. Expert Rev. Anti. Infect. Ther. 3, 805–814.

Burba, I., Colombo, G.I., Staszewsky, L.I., *et al.* (2011). Histone deacetylase inhibition enhances self renewal and cardioprotection by human cord blood-derived CD34 cells. PLoS One 6, e22158.

Christian, M., Cermak, T., Doyle, E.L., *et al.* (2010). Targeting DNA double-strand breaks with TAL effector nucleases. Genetics 186, 757–761.

Cong, L., Ran, F.A., Cox, D., *et al.* (2013). Multiplex genome engineering using CRISPR/Cas systems. Science 339, 819–823.

Cornu, T.I., and Cathomen, T. (2007). Targeted genome modifications using integrase-deficient lentiviral vectors. Mol. Ther. 15, 2107–2113.

Huber, K., Doyon, G., Plaks, J., *et al.* (2011). Inhibitors of histone deacetylases: Correlation between isoform specificity and reactivation of HIV type 1 (HIV-1) from latently infected cells. J. Biol. Chem. 286, 22211–22218.

Joglekar, A.V., Hollis, R.P., Kuftinec, G., *et al.* (2013). Integrase-defective lentiviral vectors as a delivery platform for targeted modification of adenosine deaminase locus. Mol. Ther. 21, 1705–1717.

Kaur, K., Mirlashari, M.R., Kvalheim, G., and Kjeldsen-Kragh, J. (2013). 3′,4′-Dimethoxyflavone and valproic acid promotes the proliferation of human hematopoietic stem cells. Stem Cell Res. Ther. 4, 60.

Knipe, D.M., Lieberman, P.M., Jung, J.U., *et al*. (2013). Snapshots: Chromatin control of viral infection. Virology 435, 141–156.

Lieberman, P.M. (2008). Chromatin organization and virus gene expression. J. Cell Physiol. 216, 295–302.

Lombardo, A., Genovese, P., Beausejour, C.M., *et al*. (2007). Gene editing in human stem cells using zinc finger nucleases and integrase-defective lentiviral vector delivery. Nat. Biotechnol. 25, 1298–1306.

Margolis, D.M. (2011). Histone deacetylase inhibitors and HIV latency. Curr. Opin. HIV AIDS 6, 25–29.

Naldini, L., Blömer, U., Gage, F.H., *et al*. (1996). Efficient transfer, integration, and sustained long-term expression of the transgene in adult rat brains injected with a lentiviral vector. Proc. Natl. Acad. Sci. U.S.A. 93, 11382–11388.

Nightingale, S.J., Hollis, R.P., Pepper, K.A., *et al*. (2006). Transient gene expression by nonintegrating lentiviral vectors. Mol. Ther. 13, 1121–1132.

Pelascini, L.P., Janssen, J.M., and Gonçalves, M.A. (2013a). Histone deacetylase inhibition activates transgene expression from integration-defective lentiviral vectors in dividing and non-dividing cells. Hum. Gene Ther. 24, 78–96.

Pelascini, L.P., Maggio, I., Liu, J., *et al*. (2013b). Histone deacetylase inhibition rescues gene knockout levels achieved with integrase-defective lentiviral vectors encoding zinc-finger nucleases. Hum. Gene Ther. Methods 24, 399–411.

Staunstrup, N.H., and Mikkelsen, J.G. (2011). Integrase-defective lentiviral vectors—a stage for nonviral integration machineries. Curr. Gene Ther. 11, 350–362.

Takacs, M., Banati, F., Koroknai, A., *et al*. (2010). Epigenetic regulation of latent Epstein-Barr virus promoters. Biochim. Biophys. Acta 1799, 228–235.

Urnov, F.D., Miller, J.C., Lee, Y.L., *et al*. (2005). Highly efficient endogenous human gene correction using designed zinc-finger nucleases. Nature 435, 646–651.

Van Lint, C., Emiliani, S., Ott, M., and Verdin, E. (1996). Transcriptional activation and chromatin remodeling of the HIV-1 promoter in response to histone acetylation. EMBO J. 15, 1112–1120.

Vargas, J., Jr., Gusella, G.L., Najfeld, V., *et al*. (2004). Novel integrase-defective lentiviral episomal vectors for gene transfer. Hum. Gene Ther. 15, 361–372.

Address correspondence to:
Dr. Donald B. Kohn
3163 Terasaki Life Science Bldg
610 Charles E. Young Drive South
Los Angeles, CA 90095

E-mail: dkohn@mednet.ucla.edu